Offshore Meteorology for Multi-Mega-Watt Turbines

Jens Tambke[1], Lorenzo Claveri[2], John A.T. Bye[3], Carsten Poppinga[1],
Bernhard Lange[4], Lueder von Bremen[1], Francesco Durante[5], Jörg-Olaf Wolff[6]

[1]ForWind - Center for Wind Energy Research,
Institute of Physics, University of Oldenburg, 26111 Oldenburg, Germany
e-mail: jens.tambke@mail.uni-oldenburg.de, Tel. +49-441-36116736, www.energiemeteorologie.de

[2]FMI, Finnish Meteorological Institute, Helsinki, Finland
[3]School of Earth Sciences, The University of Melbourne, Victoria 3010, Australia
[4] formerly [1]ForWind, now ISET e.V., University of Kassel, 34119 Kassel, Germany
[5]DEWI, German Wind Energy Institute, Wilhelmshaven, Germany
[6]Physical Oceanography (Theory), ICBM, University of Oldenburg, 26111 Oldenburg, Germany

Abstract

To achieve precise wind resource assessments, to calculate loads and wakes as well as for reliable short-term wind power forecasts, the vertical wind profile above the sea has to be modelled with high accuracy for tip heights up to 160m. For these purposes, it is crucial to consider the special meteorological characteristics of the marine atmospheric boundary layer. Continuing our work in the EU-project ANEMOS [1], we analysed marine wind speed profiles that were measured at the two met masts Horns Rev (62m high) and FINO1 (103m) in the North Sea. We found pronounced effects of thermal stratification and of the influence of the land-sea transition. In many situations, the wind shear is significantly higher than expected with standard approaches in mesoscale models. Nevertheless, the numerical analysis of the marine wind field above the North Sea from the German Weather Service seems to provide a good assessment of wind speeds at 103m height.
For an improved simulation of the vertical wind speed profiles, we developed a new analytic model of marine wind velocity profiles. In particular, the flux of momentum through the Ekman layers of the atmosphere and the sea is described by a common wave boundary layer. The good agreement between our theoretical profiles and observations at Horns Rev and FINO1 support the basic assumption of our model that the atmospheric Ekman layer begins at 10 to 30m height above the sea surface.

Key words: Offshore Wind Resource Assessment; Marine Meteorology; Wind Speed Profile; Ekman Layer

1. Introduction

In contrast to wind flow conditions over land the meteorological situation offshore is different mainly due to three important effects:
1) The non-linear wind-wave interaction leads to a variable, but small surface roughness.
2) The large heat capacity of the water strongly affects the spatio-temporal characteristics of the thermal stratification of the air.
3) Internal boundary layers caused by the land-sea discontinuity modify the structure of the marine atmospheric flow.
Previous investigations for sites in the Baltic Sea showed that these meteorological conditions over the sea strongly influence offshore wind profiles [2,3]. The wind conditions above the North Sea are expected to differ from those of the Baltic Sea owing to the long fetches, i.e. to the large distances to the nearest coast in most wind directions. These fetches of several hundred kilometres are expected to lead to decreased turbulence intensities. This feature influences the whole structure of the marine wind field, which is not sufficiently understood so far.

Figure 1: Satellite image of the North Sea, showing the positions of the FINO1 and Horns Rev measurement sites

2. Offshore Wind Profiles at Horns Rev

The meteorological mast at Horns Rev is located approximately 18km west of Blaavands Huk at the Danish North Sea coast and is operated by Elsam Engineering A/S [4]. We investigated the period from 10/2001 till 04/2002 for which the wind speed measurements in four heights (15m, 30m, 45m and 62m) are available. Air temperatures were measured at 13m and 55m above, the water temperature at 4m below the mean sea level (DNN). The measurement data is provided by the Database on Wind Characteristics (www.winddata.com). The data set contains about 23 000 records of 10-minute mean values.

In order to correct the wind speeds at 15m, 30m and 45m for flow distortion of the lattice mast, we applied a linear correction model developed by Hoejstrup [5] and Lange [6]. To determine the correction coefficients, we analysed the wind speed ratios of the two cup anemometers on each side of the mast depending on the wind direction. The effect of dynamic pressure directly in front of the mast is modelled by a correction factor u(measured) / u(undisturbed) = 0.993, whereas the maximum overspeeding near the wake of the mast leads to a factor of 1.041. From the two installed anemometers the one more in front of the mast (depending on wind direction) was selected for the investigations.

In the first half of the given period, the water temperature is on average higher than the air temperature, whereas it is vice versa in the second half. Therefore, all thermal situations can be expected to occur. There was no information available on the accuracy of the calibration of the temperature sensors Thus, it is uncertain whether a potential temperature difference close to zero, i.e. in the range -0.05 to +0.05 Kelvin, really denotes neutral conditions of the thermal stratification. For that reason, we characterized all observed thermal situations by the wind speed ratios between different heights.

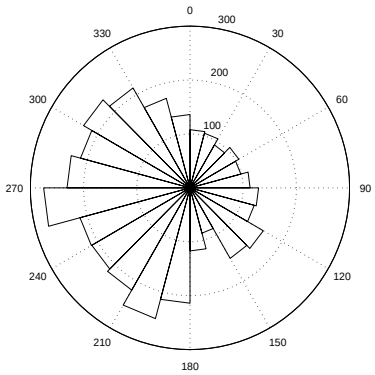

Figure 2: Frequency of wind directions in 43m height at Horns Rev in arbitrary units. Main wind directions: westerly winds from sea to land; Winter period 10/2001 till 04/2002

2.1 Dependence on wind direction

At Horns Rev, winds are mainly coming from the open North Sea with fetches of several hundred kilometres (*Figure 1* and *Figure 2*).

In *Figure 3* and *Figure 4* the average profiles for different wind directions are shown. As expected the highest wind speeds are observed for the two sectors where the wind blows from westerly directions over the open sea, i.e. 225° to 315°. In these cases the strong winds generated by typical low pressure systems are not decelerated by land masses. In contrast to this, north-easterly winds (0° - 90°) which are mostly due to high pressure systems related to low wind speeds approach the site via the mainland of Denmark. Consequently, the corresponding measured profiles have considerably lower wind speeds. Finally, southerly and north-westerly winds (90° - 225° and 315° - 360°) have medium wind speeds.

Note that the height in *Figure 3* and *Figure 4* is plotted in a logarithmic scale. The standard logarithmic profile which would be expected in neutral situations would appear here as a straight line. In most sectors the measured profiles deviate from a logarithmic shape by higher wind shears. The supralogarithmic deviations are most pronounced for the five sea sectors with purely marine winds from the west (135° - 360°) where the profiles seem to be logarithmic up to 45m, but at 62m the measured wind speed is on average about 0.3 m/s higher than it would be estimated by a logarithmic extrapolation from the lower heights.

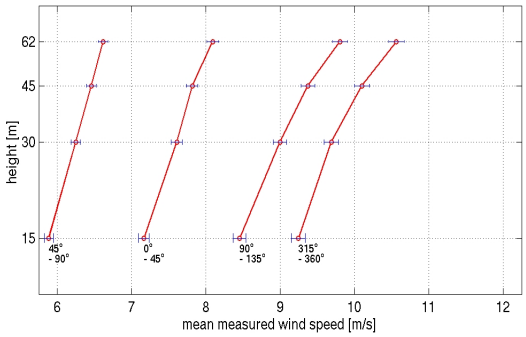

Figure 3: Mean measured profiles at Horns Rev for different northerly and easterly wind directions from 315° to 135°. Logarithmic scale of height.

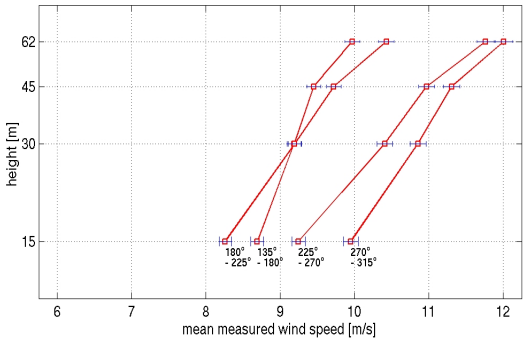

Figure 4: As Fig. 3, but for different southerly and westerly wind directions from 135° to 315°.

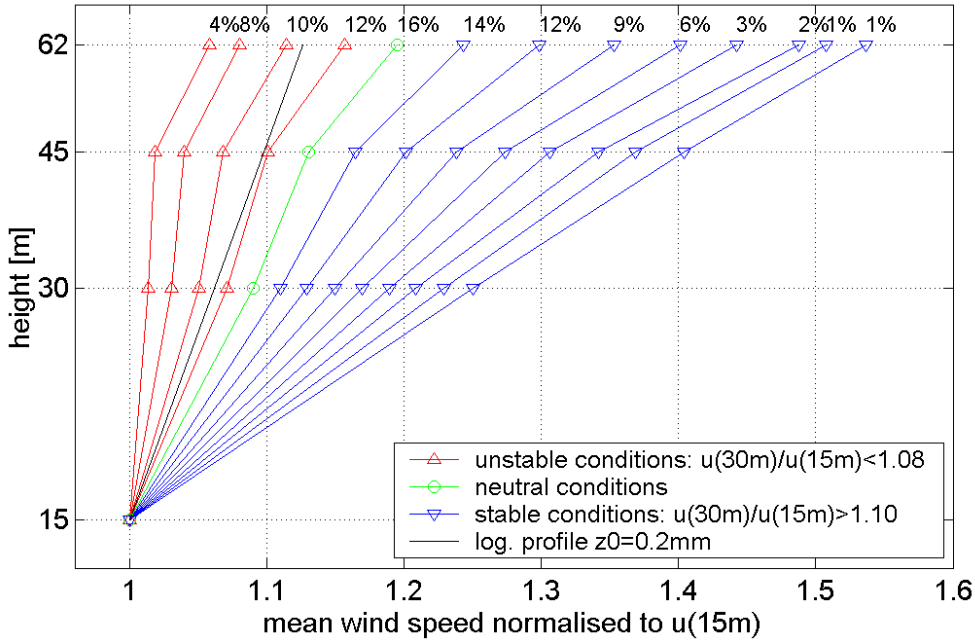

Figure 5: Bin averages of relative mean measured wind speed profiles at Horns Rev, normalised to the speed at 15m height, for wind speeds between 5m/s and 30m/s (=maximum) at 62m height and wind directions from 135° to 360°. The profiles are bin averaged according to the wind speed ratio between 30m and 15m height as an indicator for the thermal stability of the flow. Period 10/2001-04/2002. The percentages show the frequency of occurrence of each profile bin. Top Figure: Logarithmic scale of height. Small Figure: Linear scale.

2.2 Dependence on thermal stratification

The observed supralogarithmic deviations could be easily explained with a stable thermal stratification of the boundary layer. But remarkably, this 'bending' to higher wind speeds at 62m height occurs in all thermal conditions that were observed at Horns Rev: *Figure 5* shows the normalised mean measured wind profiles from the sea sectors for the full range of observed wind speed ratios between 15m and 30m height, together with the frequency of the respective occurrence. The neutral range with u(30m)/u(15m) between 1.08 and 1.10 and with u(62m)/u(15m) between 1.17 and 1.22 was determined from the narrow range of wind speed ratios for wind speeds higher than 18m/s at 15m height. Here we considered that for lower wind speeds the neutral ratio should be lower due to the increase of sea surface roughness with wind speed like in the standard Charnock relation (z0=0.0185*(u_*^2)/g). However, a standard logarithmic profile with an offshore roughness length of z0=0.2mm or calculated with the Charnock relation leads only to wind speed ratios of 1.05 to 1.08 between 15m and 30m and of 1.11 to 1.16 between 15m and 62m height (in the speed interval of u(15m) from 5m/s to 25m/s).

Nevertheless, *Figure 5* shows that the thermal stratification leads to very different wind speed ratios. The thermally influenced wind speed profile in the atmospheric surface layer is commonly described by Monin-Obukhov similarity theory. In homogeneous and stationary flow conditions, it predicts a log-linear profile:

$$u(z) = \frac{u_*}{\kappa}\left[\ln\left(\frac{z}{z_0}\right) - \Psi_m\left(\frac{z}{L}\right)\right]$$

The wind speed u at height z is determined by friction velocity u_*, aerodynamic roughness length z_0 and Monin-Obukhov length L. κ denotes the von Karman constant (taken as 0.4) and Ψ_m is a universal stability function. We use the Businger-Dyer formulation [7] of the stability function with parameters of the reanalysis by Högström [8].

If the wind speed is known at one height, the vertical wind speed profile is determined by two parameters: the surface roughness z_0 and the Obukhov length L. Here, a constant roughness of z_0=0.2mm is used. The Obukhov-length L is calculated from the bulk Richardson number Rib between the sea surface and 15m height with the widely implemented formulas

from Grachev and Fairall [9]. Rib has proved to be a stability measure that is robust against small errors in the temperature sensor calibration.

$$Rib = \frac{g}{T}\frac{z\Delta\theta_v}{U^2}$$

where g is the acceleration of gravity, T the absolute temperature at z = 15m height, U is the wind speed at 15m height, and $\Delta\theta_v$ ist the virtual temperature difference between the air at 15m height and the sea surface, which is a function of the difference between the measured temperatures of the air and the water Tair(13m)-Tsea(-4m), see [9].

A comparison of the measured wind shear with the predictions of Monin-Obukhov theory is made by plotting the measured wind speed ratio at two heights versus the stability parameter 10m/L, *Figure 6*. Here the heights of 62m and 15m were chosen. Only records with wind speeds above 5m/s have been used to avoid increased scatter.

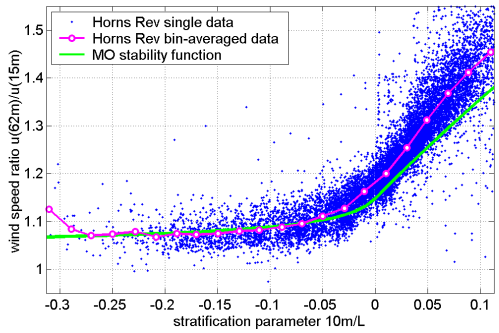

Figure 6: Ratios between measured wind speeds at 62m and 15m height depending on the inverse of the Obukhov length L as a measure of thermal stability of the atmospheric flow at Horns Rev. Data set as in Figure 5.

Figure 6 shows that the wind speed ratios at Horns Rev clearly exceed those predicted with the Monin-Obukhov stability functions for neutral and stable situations (10m/L >= 0). Similar results were found by Lange [2] for the Baltic Sea, but with relatively small fetches to the coastline (10-50 km).

Deviations of offshore profiles from the logarithmic profile caused by internal boundary layers (IBL) related to the land-sea discontinuity have been observed for sites in the Baltic Sea [6]. But this is no explanation for the sea sector profiles at Horns Rev as the fetches of 500 to 800km seem to be far too long for this sort of IBL to sustain.

The observed effect of supralogarithmic wind shears at Horns Rev might be explained with the special meteorological conditions at sea. In particular, the low turbulence might decrease the height of the surface layer such that the logarithmic wind profile looses its validity in lower heights compared to onshore and the anemometers at 30m and 45m height are already located in the Ekman layer. The linear plot in the small *Figure 5* reveals that the supralogarithmic bending is in fact an almost linear increase of the wind speed, which is more similar to the wind shear in the Ekman layer.

In contrast to this, it is possible that the applied correction for flow distortion due to the lattice mast is not sufficient. Therefore, we looked for a direction dependency of the deviations by comparing small sectors (±15°) around the wind direction where the mast is directly behind the anemometer to directions where the anemometers are besides the mast. In all cases the profiles show the same difference from the standard MO-corrected logarithmic shape. In addition, measurements carried out on a mast of the same type located at Læsø wind farm in the Baltic Sea and also operated by ELSAM do not show an increased wind speed recorded on top of the mast [4]. Hence, a systematic error due to the geometry of the mast is not detected. Nevertheless, the possibility remains that the measurement procedure influences the observed effects.

3. Offshore Wind Profiles at FINO1

The FINO1 measurement platform [10] is located 45km north of the island of Borkum in the North Sea (see Fig. 1). Eight cup anemometers are installed at heights of 33m to 103m, those from 33m to 91m on booms mounted in south-east direction of the mast. Three ultrasonic anemometers are present at heights of 41m, 61m, and 81m on north-westerly oriented booms. Additional meteorological measurements consist of wind direction, air and water temperature, moisture, air pressure and solar irradiation.

Data from January to December 2004 have been used in this study. The data set contains about 70.000 records of 10-minutes average values.

The first results support the Horns Rev findings of almost linear wind shears for south-westerly winds (190°-250°) for all classes of thermal stratification (*Figure 7*). The effect of the mast for other wind directions could not be completely corrected yet.

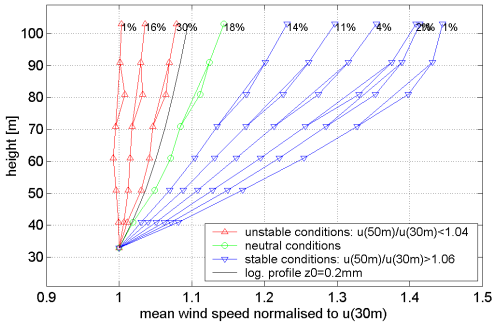

Figure 7: Bin averages of relative mean measured wind speed profiles at FINO1, normalised to the speed at 33m height, for wind speeds between 4m/s and 30m/s (=maximum) at 100m height and wind directions from 190° to 250°. The profiles are bin averaged according to the wind speed ratio between 51m and 33m height as an indicator for the thermal stability of the flow. The neutral ratio was determined from situations with wind speeds higher than 20m/s at 30m height. The anemometer at 81m height is known for overspeeding. Period 01-12/2004. Linear scale of height. Black: Percentage of occurrence.

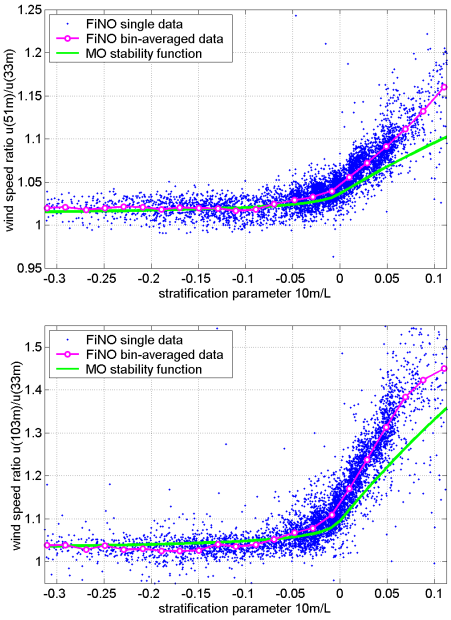

Figure 8: Measured ratio between the wind speeds at 103m and 33m (top figure) and between 51 and 33m height (bottom) versus stability parameter 10m/L at FINO1. Data set as in Figure 7.

The wind speed ratios that could be identified as neutral are similar to those at Horns Rev (comparable ratios between 30m and 62m). They are clearly higher than in the logarithmic profile with z0=0.2mm (the best fit can be achieved at both sites with z0=1cm). As in the previous section, we calculated the bulk Richardson number also for the FINO-data. In contrast to Horns Rev, we used the speed and temperature sensors at 41m height, which can be accounted for with the formulaes in [9] when deriving the stability parameter 10m/L. Again, only records with wind speeds above 5m/s have been used to avoid increased scatter. *Figure 8* shows the results for the FINO1 site, their bin averages and the prediction with Monin-Obukhov stability functions from [7] and [8]. Like at Horns Rev, the measured wind speed ratios clearly exceed those from common theory for neutral and stable situations.

In ongoing studies, we analyse alternative ways to determine the thermal stability, especially based on the sonic measurements which are currently recalibrated.

4. Comparison of MM5 and DWD-Analysis at FINO1

Apart from the 1-dimensional micrometeorological analysis, we made a first evaluation of mesoscale-model simulations. Here we compared the Analysis data of the German Weather Service (7km horizontal resolution, prognostic levels at 34m and 110m, www.dwd.de) and our own MM5-simulation, based on NCEP/NCAR Reanalysis data (2.5° resolution) as initial and boundary conditions. In MM5, three nested domains have been used, with horizontal resolutions of 81, 27 and 9km, respectively, and one-way nesting. The number of sigma levels in the vertical direction has been limited to 24 and the ETA Mellor-Yamada-Janjic PBL scheme was used.

Figure 9 shows the mean measured profile (average in year 2004) for the undisturbed sector 190°-250°, compared to the mean profiles produced by the DWD-model and MM5 in that year for the same sector 190°-250°. Both models reproduce the observed mean wind speed at 103m height, but show considerably lower wind shears than the measurement. When evaluating the full time series at 103m, i.e. for the whole year 2004 and all wind directions, MM5 shows a mean 103m wind speed of only 9.3m/s, whereas the DWD reproduces correctly the mean measured wind speed of 9.8m/s.

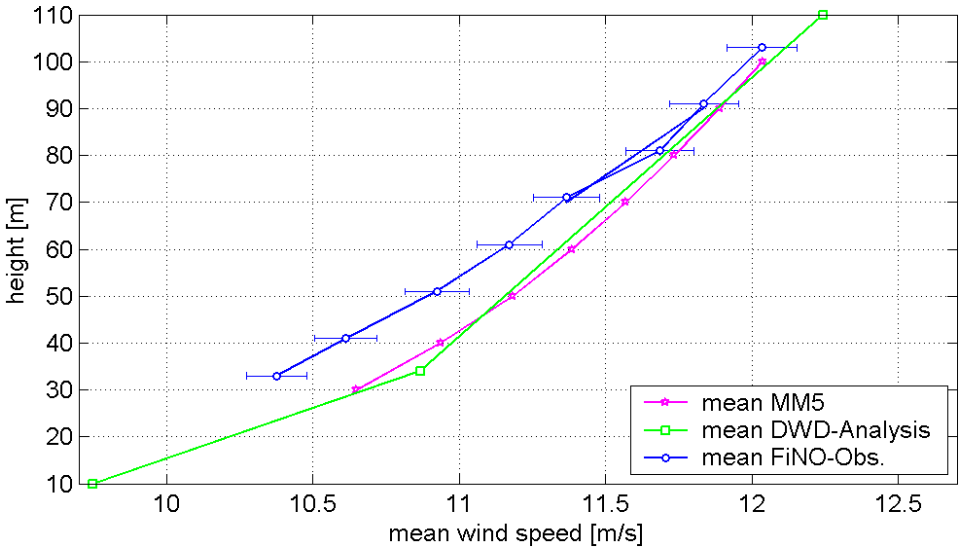

Figure 9: Mean measured sea sector (190° - 250°) wind profile at FINO1 in 2004 compared to the mean output of two mesoscale simulations for the same wind directions: DWD-Analysis and MM5-Simulation (based on NCEP/NCAR Reanalysis).

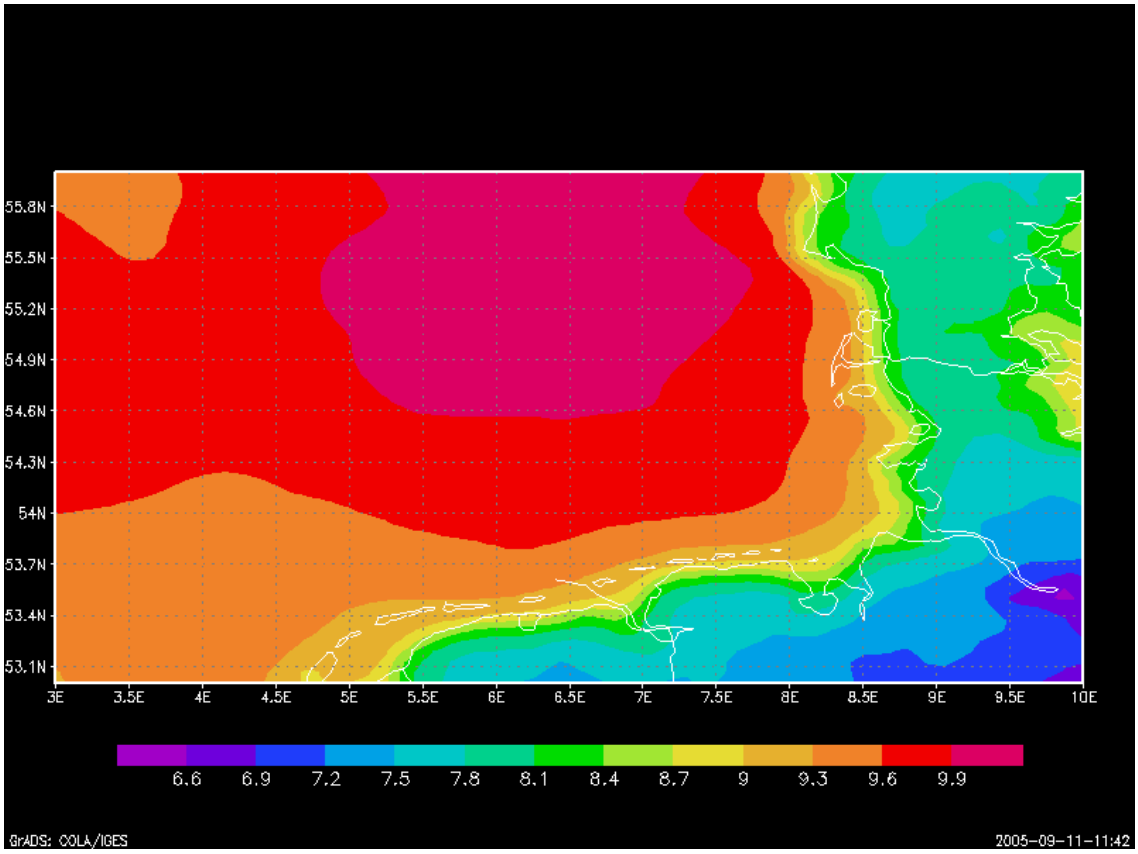

Figure 10: Mean 103m wind speeds in the German Bight in 2004, calculated from the DWD-Analysis.

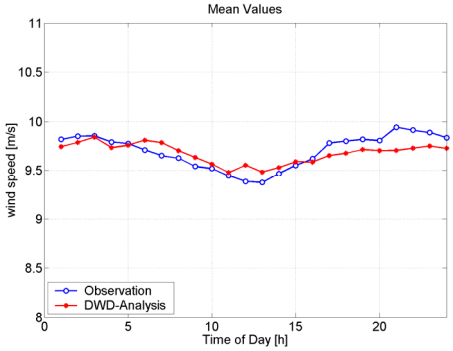

Figure 11: Mean 103m wind speeds at FINO1 for different times of the day, year 2004.

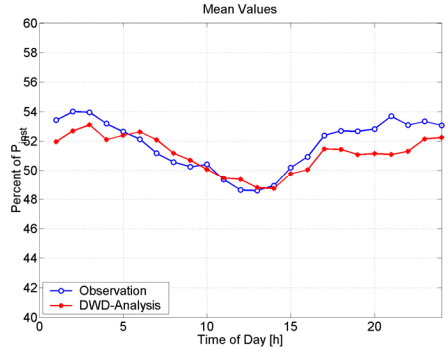

Figure 13: Mean calculated power output at FINO1 for different times of the day, year 2004.

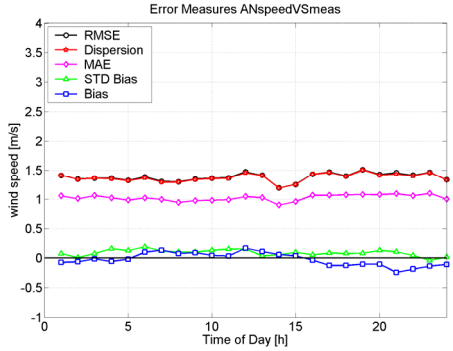

Figure 12: Error measures of wind speeds from DWD-Analysis against FINO1-Obs for different times of the day, year 2004.

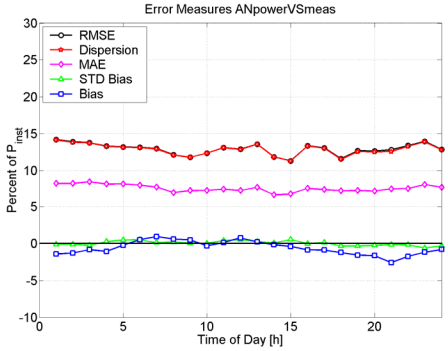

Figure 14: Error measures of calculated wind power from DWD-Analysis against FINO1-Obs for different times of the day, year 2004.

Figure 12 shows that the BIAS and the STDBIAS (difference of standard deviations of both time series) of the DWD-Analysis are negligible. The small RMSE of 1.4m/s is fully determined by the dispersion (phase or correlation) error.
When we multiply the time series of wind speed with a typical multi-mega watt power curve, the mean diurnal variation of the wind speeds leads to a more pronounced variation of the mean power output between 48% and 54% of the installed capacity (Fig 13). The RMSE of the modelled power time series is 13% of the installed capacity (Fig14).

5. Theory of inertially coupled wind profiles

For a better simulation of offshore wind profiles than shown in *Figure 9* we have developed an alternative vertical wind profile model that is based on inertial coupling between the Ekman layer of the atmosphere and the currents of the sea introduced by Bye in [11] and [12] and explained in detail in [13].
As usual the geostrophic wind is regarded as the driving force of the wind field in lower layers of the atmosphere. The momentum is transfered downwards through the Ekman spiral which is defined by a constant turbulent viscosity [14]. Similar to the Ekman layer of the air there is an Ekman layer of the water below the sea surface.
The important point addressed here is to derive an adequate description of the coupling between the two Ekman layers where the idea is to introduce a wave-boundary layer with a logarithmic wind profile that reaches only up to a maximal height of 30m. The momentum transport from the wind flow into the ocean and hence, the wind profile crucially depend on these coupling relations between the three flow layers.

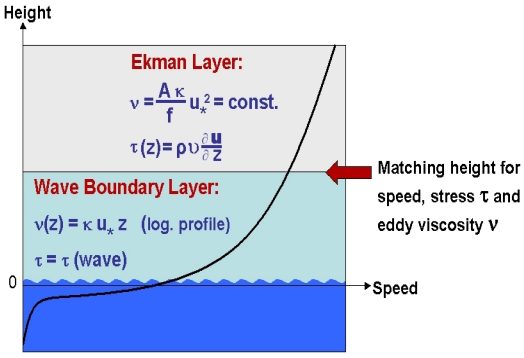

Figure 15: Scheme of the vertical wind profile used in the ICWP model.

5.1 Basic assumptions

In order to derive the coupling relations, the following assumptions are made.
First, close to the wave surface the ratio between the drift velocities of air, u_{air}, and water, u_{water}, is given by the square root of the inverse density ratio of the two fluids. The same holds for the ratio between the friction velocities:

$$\frac{u_{\text{water}}}{u_{\text{air}}} = \frac{w_*}{u_*} = \sqrt{\frac{\rho_{\text{air}}}{\rho_{\text{water}}}} \qquad (1)$$

where u_* is the friction velocity of the air flow and w_* the one of water flow while ρ_{air} and ρ_{water} are the respective densities. This is equivalent to assuming that the shear stress is continuous across the interface between air and water.
The inertial coupling relation [11] determines this shear stress at the sea surface in a drag law:
τ (wave)=$K_I(\sqrt{\rho_{air}}\ u_{air} - \sqrt{\rho_{water}}\ u_{water})^2$,
where K_I is a drag coefficient.
Second, the layer connecting the two Ekman layers of atmosphere and ocean is assumed to have a constant shear stress and will be denoted as wave-boundary layer extending from a height z_B above to $-z_B$ below the water level. This layer is similar to the surface layer onshore where the logarithmic wind profile is valid. Third, analoguous to the similarity relation (1) the turbulent viscosities, ν_{air} and ν_{water} of the two Ekman layers are also assumed to be weighted according to the inverse density ratio of the two fluids:

$$\frac{\nu_{\text{water}}}{\nu_{\text{air}}} = \frac{\rho_{\text{air}}}{\rho_{\text{water}}} \qquad (2)$$

As shown by Bye [12] these physically justified conditions allow the determination of the velocities of the two fluids at certain heights dependent on a given geostrophic wind. The full profiles can then be derived in the following way.
Due to the constant shear stress the wind profile in the wave-boundary layer has a logarithmic shape. Expressed in a coordinate system where the horizontal component of the stress tensor $\vec{\tau}_h$ is parallel to the x-axis the profile can be written as

$$\vec{u}(z) = \left(u_{\text{L}} + \frac{u_*}{\kappa} \ln\left(\frac{z}{z_{\text{R}}}\right), v_{\text{L}} \right) \qquad (3)$$

and is valid for $z_R \le z \le z_B$. κ is the von Karman constant and z_R is the height where the momentum transfer from the air to the wave field is centred. As a result of the above assumptions and the choice of the coordinate system the 'offset' (u_L, v_L) is directly given by the geostrophic wind $\vec{G} = (u_g, v_g)$, see the theory in [12]:

$$(u_{\text{L}}, v_{\text{L}}) = \frac{1}{2}\vec{G} \qquad (4)$$

Note that in the chosen coordinate system $u_g > 0$ and $v_g < 0$.
The relation that connects the friction velocity u_* at the water surface to the geostrophic wind is given by

$$|\vec{G}| = \frac{\sqrt{r^2+1}}{|r+1|}\frac{u_*}{\sqrt{K_I}} \quad (5)$$

where K_I is the drag coefficient of the wave-boundary layer The angle of rotation of the surface stress tensor to the left hand side of the geostrophic velocity (in the northern hemisphere) is *atan(-1/r)* with *-1 < r < -infinity*, where *r* still has to be determined.

The height of the wave-boundary layer z_B can be related to the wave field. Previous results from oceanography suggest that z_B is reciprocal to the peak wave number, k_p, of the wave spectrum [15]. The corresponding peak wave velocity, c_p is given by $c_p = \sqrt{g/k_p}$ where g is the gravitational constant. Assuming that c_p is proportional to the wind speed $u(z_B)$, i.e. $c_p = B\ u(z_B)$, the height of the wave-boundary layer can be written as

$$z_B = \frac{B^2}{8g}\frac{(2r+1)^2}{r^2+1}|\vec{G}|^2 \quad (6)$$

The factor B has been determined from empirical data by Toba [16]. For heights above z_B the velocity vector in the Ekman layer is described by an Ekman spiral

$$u(\hat{z}) = \hat{u}_1[\cos(\beta\hat{z}) - \sin(\beta\hat{z})]e^{-\beta\hat{z}} + u_g \quad (7)$$

$$v(\hat{z}) = \hat{v}_1[\cos(\beta\hat{z}) + \sin(\beta\hat{z})]e^{-\beta\hat{z}} + v_g \quad (8)$$

with $\hat{z} = z - z_B$ and $\beta = \sqrt{f/(2\hat{\nu})}$ where f is the Coriolis parameter, $\hat{\nu}$ is the turbulent viscosity, $\hat{u}_1 = 0.5\ u_g/r$ and $\hat{v}_1 = -0.5\ v_g$.

At the interfaces between wave-boundary layer and Ekman layer, i.e. $z = \pm z_B$, the turbulent stress tensor and the turbulent viscosity is assumed to be continuous such that the wind profiles can be matched smoothly. This matching condition at the transition between wave-boundary layer and Ekman layer provides the necessary link to calculate the parameter r. At $z = z_B$ the height dependent viscosity

$$\nu(z_B) = \kappa u_* z_B \quad (9)$$

of the wave-boundary layer and the constant viscosity

$$\hat{\nu} = \frac{2}{f}(r+1)^2 K_I u_*^2 \quad (10)$$

of the Ekman layer are set equal, i.e. $\nu(z_B) = \hat{\nu}$. Using equations (5) and (6) this provides the defining equation for r:

$$-|\vec{G}|\sqrt{K_I}\left(\frac{B}{4K_I}\right)^2\kappa\left(\frac{f}{g}\right)\frac{(2r+1)^2}{(r+1)^3\sqrt{r^2+1}} = 1 \quad (11)$$

The parameters $K_I = 1.5 \times 10^{-3}$ and $B = 1.3$ can be obtained from oceanographic measurements [12,16,17], f and g are known constants at the desired location and the geostrophic wind $\vec{G}$ as driving force can be chosen to match the input of a given wind speed at a specific height. Hence, equation (11) can be iteratively solved for r and the vertical wind profiles according to equations (3) and (7,8) can be calculated. These profiles will be denoted ICWPs.

An extension with Monin-Obukhov similarity theory is straight forward: The universal stability function $\Psi_m(z/L)$ is introduced in eq. (3) and leads to an additional factor $\Phi(z_B/L)$ on the right side of eq. (9) and accordingly on the left side of eq. (11). The problem then is to calibrate the new stability function $\Phi(z/L)$ with the Obukhov length L from observations.

5.2 Comparison with measurements at Horns Rev and FINO 1

The wind speed profiles according to ICWP theory are calculated such that the wind speeds at 30m height correspond to the measurement at that height.

In *Figure 16* the mean measured sea sector wind profile (135°-360°) at Horns Rev and the corresponding mean of the ICWP profiles are compared. Taking into account that the only information given to the ICWP model is the wind speed at 30m, the mean wind shear is covered remarkably well which is related to the non-logarithmic shape of the ICWP due to the Ekman part of the profile (equation (7,8)). The wind speed at 62m is almost captured (*bias* = 0.1m/s). The root mean square error RMSE for the whole time series amounts to 6.1 % of the wind speed at 62m height. This is due to the scatter of measured wind speed ratios as a result of the variability caused by the thermal stratification.

Figure 17 shows the same comparison for FINO1. The mean wind shear at FINO1 is reproduced very precisely for wind speeds between 4m/s and 30m/s. The relative RMSE of the ICWPs over the full time series is 5% at 61m height and 10% at 103m.

These results have been obtained without the Monin-Obukhov correction in the ICWPs, because Rib (or L) is only known for parts of the time series due to the lack of continuous temperature measurements. But when the MO-extended ICWP model is provided with the information about the particular wind speed ratios between 33m and 51m height as an alternative stability measure, the RMSE at 103m height is reduced to 3.6%.

At both sites, the standard offshore WAsP profile underestimates the wind shear, even though it includes a correction for a slightly stable climate [18].

These preliminary results require further analysis of modelled *and* measured profiles, especially regarding thermal conditions and the corrections for mast flow distortion, which seem to be problematic, especially for 81m height.

The calibration of the air temperature sensors and of the flux measurements with the ultra sonic anemometers are now the most important task in order to allow for an accurate determination and modelling of the thermal stability.

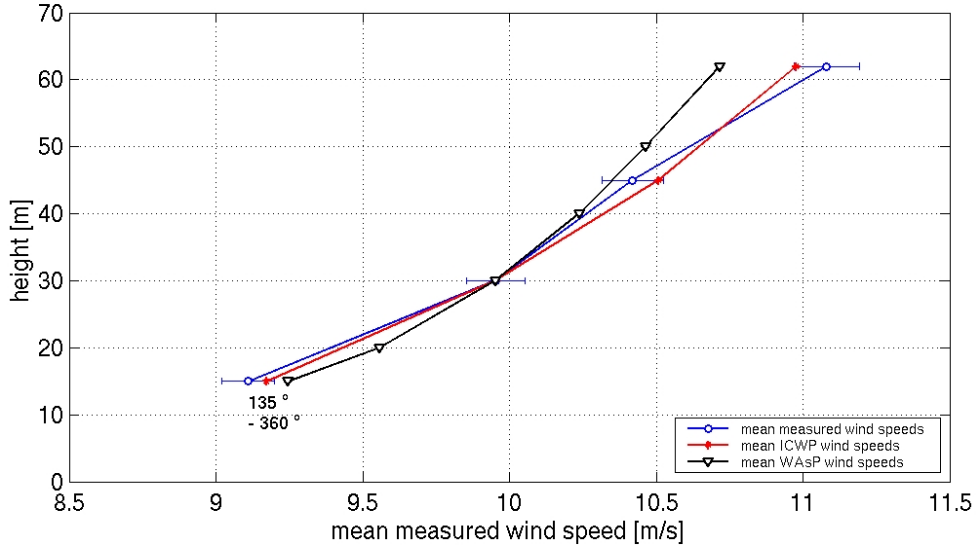

Figure 16: Mean measured "open sea" sector (135° - 360°) wind profile at Horns Rev compared to mean of ICWPs and average offshore WAsP profile.Period 10/2001-04/2002.

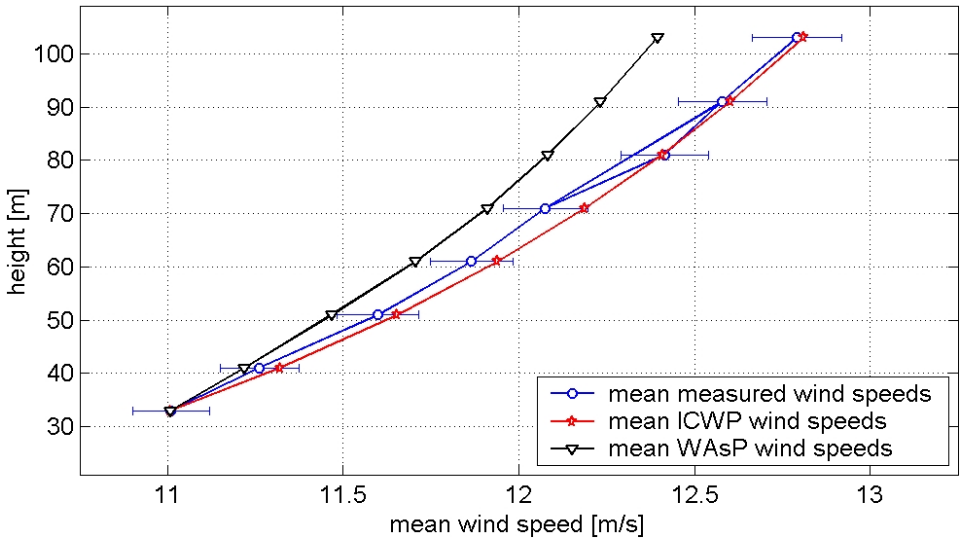

Figure 17: Mean "open sea" wind profiles at FINO 1 for the undisturbed sector (190° - 250°) and wind speeds greater than 4 m/s at 100m height: Obs. compared to mean of ICWPs and average offshore WAsP profile. Year 2004.

6. Conclusions

Our analysis shows that the offshore profiles measured at Horns Rev and FINO1 deviate considerably from the expected shapes by higher wind shears. A meteorological reason might be found in a thinner logarithmic layer than onshore and a lower onset of the atmospheric Ekman layer. Further measurements are necessary to confirm our findings.

We introduce an alternative way to describe the vertical wind profile over the sea which is based on inertially coupling the Ekman layers of air and sea with a wave-boundary layer with constant shear stress in between. For wind directions with long fetches the profiles derived by this method are in good agreement with the mean measured wind shears. In general, inertially coupled wind profiles (ICWPs) seem to be a promising approach with good potential to be further improved.

The wind speed Analysis of the German Weather Service proves to be a good candidate for a micrometeorological vertical refinement using the ICWP-theory in order to calculate the potential power output of future offshore wind farms.

Future work has to focus on describing thermal air-sea interactions and fetch-dependent influences in

order to improve both the description of wind profiles and the numerical prediction models, see [1,19]. Most important, thermal stratification has to be measured more precisely to allow a detailed modelling.

7. Acknowledgements

We like to thank www.winddata.com, Germanischer Lloyd, DEWI and DWD for providing the data. This work was funded by the European Commission (ANEMOS project, http://anemos.cma.fr, ENK5-CT-2002-00665) and the Hanse Institute for Advanced Study, Delmenhorst.

8. References

[1] Tambke J, Bye JAT, Lange M, Focken U, Wolff J-O. Forecasting Offshore Wind Speeds above the North Sea. *Wind Energy* 2005; **8**: 3-16.

[2] B. Lange, S. Larsen, J. Højstrup, R. Barthelmie. Importance of thermal effects and sea surface roughness for offshore wind resource assessment. *Journal of Wind Engineering and Industrial Aerodynamics* **92 11** (2004) 959-998

[3] Watson SJ and Montavon C. CFD Modelling of the Wind Climatology at a Potential Offshore Farm Site. *Proc. Europ. Wind Energy Conf. EWEC*, Madrid, 2003.

[4] Sommer A. Techwise A/S. Offshore Measurements of Wind and Waves at Horns Rev and Læsø, Denmark. *In Preliminary edition for the OWEMES conference*, Naples, 2003.

[5] Højstrup J. Vertical extrapolation of offshore wind profiles. *Proc. Europ. Wind Energy Conf. EWEC*, pages 1220-1223, Nice, 1999.

[6] Lange B. Modelling the Marine Boundary Layer for Offshore Wind Power Utilisation, *volume 491 of Fortschritt-Berichte VDI Reihe 6. VDI Verlag*, Düsseldorf, 2003.

[7] Businger JA, Wyngaard JC, Izumi Y, Bradley EF. Flux-profile relationships in the atmospheric surface layer. *Journal of the Atmospheric Sciences* **28** (1971) 181-189

[8] Högström U. Non-Dimensional Wind and Temperature Profiles in the Atmospheric Surface Layer: A Re-Evaluation. *Boundary-Layer Meteorology* **42** (1988) 55-78

[9] Grachev AA and Fairall CW. Dependence of the Monin-Obukhov Stability Parameter on the Bulk Richardson Number over the Ocean. *J. Appl. Meteorol.* **36** (1997) 406-414

[10] Neumann T et al. One Year Operation of the First Offshore Wind Research Platform in the German Bight - FINO I. *German Wind Energy Conference DEWEK 2004,* Wilhelmshaven, Germany, 2004, published on CD

[11] Bye JAT. Inertial coupling of fluids with large density contrast. *Phys. Lett.* A, **202**: 222-224, 1995.

[12] Bye JAT. Inertially coupled Ekman layers. *Dyn. Atmos. Oceans*, **35**: 27-39, 2002.

[13] Tambke J, Barthelmie R, Kariniotakis G et al. Description of Offshore Prediction Models. *Report D5.1 to the European Commission, ANEMOS Project, http://anemos.cma.fr*, November 20th, 2004

[14] Ekman VW. On the influence of the earth's rotation on ocean currents. *Arkiv før Matematik, Astronomi och Fysik*, **2**: 1-53, 1905.

[15] Jones ISF and Toba Y. Wind Stress over the Ocean. *Cambridge University Press*, Cambridge, 2002.

[16] Toba Y. Local balance in the air-sea boundary process III. On the spectrum of wind waves. *J. Oceanor. Soc. of Japan*, **29**: 209-220, 1973.

[17] Garratt JR. The atmospheric boundary layer. *Cambridge University Press*, Cambridge, 1992.

[18] Mortensen NG, Landberg L, Troen I, Petersen EL. Wind Atlas Analysis and Application Program (WAsP). Risoe National Laboratory, Roskilde, Denmark, 1993.

[19] Tambke J, Poppinga C, von Bremen L, Claveri C, Lange M, Focken U, Bye JAT, Wolff J-O. Avanced Forecast Systems for the Grid Integration of 25 GW Offshore Wind Power in Germany. *Proc. Europ. Wind Energy Conf. EWEC,* Athens, 2006.